

Fabrication of YAG–SiC nanocomposites by spark plasma sintering

Lian Gao^{a,*}, Hongzhi Wang^a, Hirokazu Kawaoka^b, Tohru Sekino^b, Koichi Niihara^b

^aState Key Laboratory on High-Performance Ceramics and Superfine Microstructure, Shanghai Institute of Ceramics, Chinese Academy of Sciences, Shanghai 200050, China

^bInstitute of Scientific and Industrial Research, Osaka University, Osaka 567-0047, Japan

Received 9 November 2000; received in revised form 10 May 2001; accepted 20 May 2001

Abstract

The heterogeneous precipitation method was used to prepare YAG–5 vol.% SiC powder. Hot-press sintering and spark plasma sintering were used to obtain dense sintered bodies. The present results revealed that nanoscale-sized SiC particles were well distributed within the composites, with most of the particles located within the YAG grains. The bending strength of spark-plasma-sintered YAG–5 vol.% SiC nanocomposites was 565 MPa, much higher than that of monolithic YAG ceramics. The fracture mode of the YAG–5 vol.% SiC nanocomposites was transgranular. The present results indicate that YAG–5% SiC nanocomposites are good high-temperature structural materials and that spark plasma sintering is appropriate for fabricating high-performance YAG–5 vol.% SiC nanocomposites with a fine microstructure because the method involves a low sintering temperature. © 2002 Published by Elsevier Science Ltd.

Keywords: Mechanical properties; Nanocomposites; Sintering; YAG–SiC; Spark plasma sintering

1. Introduction

Single-crystal yttrium aluminum garnet (YAG) has the lowest creep rate of any oxide, and polycrystalline YAG also has good creep resistance at high temperature. Thus, YAG is an attractive candidate for high-temperature structural ceramics.^{1,2} However, the poor mechanical properties of polycrystalline YAG limit its application: according to some reports, hot-pressed YAG has a strength of 234 MPa, and sintered YAG has a strength of only 102 MPa.³ Thus, the mechanical properties of polycrystalline YAG must be improved before it can be applied industrially.

In the 1990s, Niihara et al.⁴ reported that incorporating nanoscale-sized particles into a ceramic matrix can increase the mechanical properties dramatically, especially in the Al₂O₃–SiC system. Those researchers believed that the mechanism of strengthening and toughening was believed to be caused by residual stresses resulting from the different thermal expansion coefficients of Al₂O₃ and SiC. Because YAG has a

coefficient of thermal expansion similar to that of Al₂O₃ and does not react with SiC, the incorporation of nanoscale-sized SiC should also efficiently improve the strength of YAG ceramics. However, few reports have been made on YAG–SiC composites.

Recently, the spark–plasma–sintering (SPS) method has been developed for fabricating metals, ceramics, and composites.^{5–9} Compared with hot-pressing, the SPS technique allows sintering at lower temperatures and with shorter soaking times. With the SPS method, raw powders in a carbon die are pressed uniaxially and a d.c. pulse voltage is applied. At an early stage of the procedure, the powders are heated by spark discharge between the particles and the carbon die is heated by the pulse voltage also. It means that all heating achieved by the spark plasma generator. Thus, the SPS method is considered suitable for fabricating fine-grained ceramics, because it effectively uses the phenomenon of microscopic electric discharge between particles under pressure. According to the Hall–Petch relationship, the strength of polycrystalline ceramics increases as grain size decreases, so that the SPS method holds promise for producing high-strength ceramics. We have used SPS to fabricate Al₂O₃–SiC nanocomposites with strength values up to 980 MPa.⁷

* Corresponding author. Tel.: +86-21-62512990; fax: +86-21-62513903.

E-mail address: liangaoc@online.sh.cn (L. Gao).

In the present study, our intention was to add nanoscale-sized SiC particles to a YAG precursor and compact this composite powder by the SPS method. Sintered bodies with fine microstructures and good mechanical properties were anticipated, because of the short sintering time and the second-phase-particle inhibition effect.

2. Experimental procedure

The heterogeneous precipitation method was used to prepare the starting powder. The processing steps for this method are outlined in Fig. 1. Aluminum nitrate [$\text{Al}(\text{NO}_3)_3 \cdot 9\text{H}_2\text{O}$, 99.0% purity], yttrium nitrate (made by dissolving Y_2O_3 into HNO_3), and nanoscale-sized SiC (average grain size, 70 nm, Institute of Chemical Metallurgy, China) were used as starting materials. The former two materials were adjusted to a 0.6 mol/l Y^{3+} and 1.0 mol/l Al^{3+} aqueous solution by dissolution in distilled water. Because the isoelectric point of an SiC aqueous suspension is located at a pH value of ~ 4 ,¹⁰ a uniformly dispersed SiC aqueous suspension was obtained by regulating the pH value to > 9 and using ultrasonic vibration. By simultaneously adding the Y^{3+} , Al^{3+} aqueous solution and ammonia to the SiC aqueous suspension, while keeping the pH value between 9 and 10, we were able to produce an $\text{Al}(\text{OH})_3$ and $\text{Y}(\text{OH})_3$ mixed precipitate that included nanoparticles of SiC. The precipitate was oven-dried at 100°C , calcined at 1100°C , and wet ball-milled to attain a YAG–SiC powder. Other researches^{4,7} have indicated that a small amount of nanoscale-sized SiC effectively toughens and strengthens the ceramic matrix. Thus, only YAG–5 vol.% SiC powder was produced in the present experiment.

The composite powders were compacted by hot-pressing (HP) and SPS, respectively. HP was conducted under 30 MPa pressure in a nitrogen–gas atmosphere, at

temperatures between 1450 and 1700°C , with a holding time of 1 h. The prepared composite powder was put in a carbon die and the sample size was $35 \times 30 \times 6$ mm.

SPS was conducted under vacuum, in a Dr. Sinter apparatus (Model No. SPS-2040, Sumitomo Coal Mining Co., Ltd., Yokohama, Japan). The prepared powder was compacted to green-body cylinders of 30 mm diameter and 10 mm height, and the cylinder was put into a carbon die having an inner diameter of 30 mm. The SPS processing parameters were as follows:

1. A pressure of 50 MPa was applied at the beginning of the sintering process and released during the cooling portion of a complete sintering cycle.
2. The pulse duration was 3.3 ms, and one pulse sequence contained 12 pulses, while the interval between pulse sequences was 6.6 ms.
3. The pulse-sequence current averaged 5000 A.
4. The sintering temperature was between 1350 and 1550°C , and the heating rate was $200^\circ\text{C}/\text{min}$.
5. The holding time at sintering temperature was 1 min.

For comparison, pure YAG powder was prepared by the coprecipitation method, with a calcination temperature of 900°C ; specific processing details are described elsewhere.¹¹ This pure YAG powder was also compacted by both HP and SPS. The sintering temperatures were 1500°C (holding time, 1 h) for HP and 1400°C (holding time, 5 min) for SPS.

Sintered sample densities were measured by the Archimedes method. For mechanical testing, the hot-pressed samples were cut and ground into rectangular bar specimens ($4 \times 3 \times 20$ mm) and measured by the three-point bend test. The fracture cross-section was examined using scanning electron microscopy (SEM), and the distribution of nanoscale-sized SiC in the YAG matrix was examined using transmission electron microscopy (TEM).

In the following discussion, the samples of YAG–5 vol.% SiC sintered by the HP and SPS methods are represented as HP YAG–SiC and SPS YAG–SiC, respectively; the samples of pure YAG sintered by the HP and SPS methods are represented as HP YAG and SPS YAG, respectively.

3. Results and discussion

3.1. Sintering behavior

The relationship between the SPS temperature and the relative density of YAG–5 vol.% SiC (Fig. 2) shows that dense sintered bodies were obtained at $> 1500^\circ\text{C}$ by the SPS method, despite a high heating rate and short soaking time. Such rapid densification results from the characteristics of SPS: the current passes

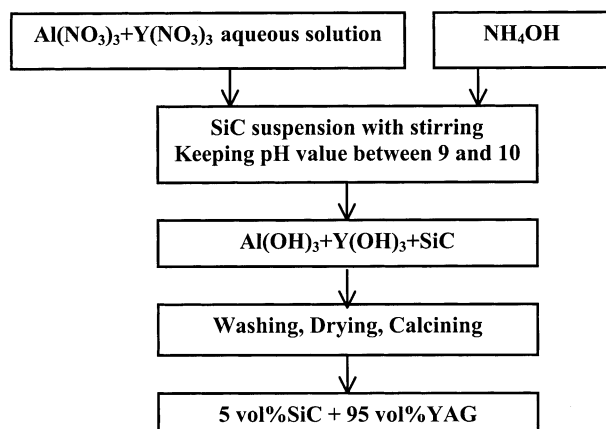


Fig. 1. Flow chart showing the fabrication of SiC–YAG powder by the heterogeneous precipitation method.

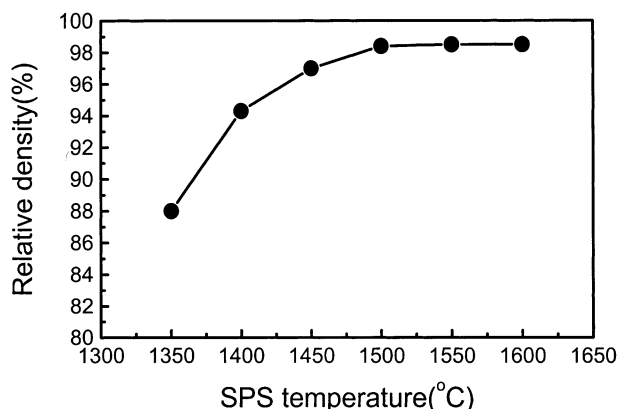


Fig. 2. Relative density versus sintering temperatures for YAG-5 vol.% SiC nanocomposites sintered by SPS.

through both the carbon dies and the sample, so that the sample is heated from both the outside and the inside resulting in a very rapid heating rate. During the initial portion of the densification process, and in connection with densification of nonconducting materials, a discharge between the particles is expected to occur; during the initial stage of each current-voltage pulse, a plasma has been reported to form.¹² Thus, these processes promote material transfer and make rapid densification of the powder compact possible at low temperatures and short holding times.

On the other hand, all of the present HP samples cracked when they were removed from the carbon die, although very slow heating and cooling rates had been applied. X-ray diffractometry results indicated that no phase transformation occurred during sintering; only two phases, YAG and SiC, were revealed in both the powder and the sintered bodies. Therefore, residual stress resulting from the different thermal expansion coefficients between the YAG and SiC seemed to cause the cracking of the sintered bodies.

Some researchers¹³ believe that the mechanical properties of Al_2O_3 -SiC nanocomposites are determined by a change in the fracture mode of Al_2O_3 when sub-micrometer-sized SiC particles are added. Calculation of the residual-stress distribution seems to indicate that the fracture mode transition is caused by the both matrix weakening and the grain-boundary strengthening. Because YAG has a thermal expansion coefficient similar to that of Al_2O_3 , the addition of nanoscale-sized SiC will also weaken the YAG matrix and strengthen the YAG grain boundary. However, the HP YAG matrix is so weak that it cannot bear the residual stresses resulting from the incorporation of SiC particles; therefore, integrated HP YAG-SiC nanocomposites are difficult to achieve.

To verify the above theory, we tested the strength of SPS YAG and HP YAG, to learn the strength of the YAG matrix in SPS YAG-SiC and HP YAG-SiC. The strength of the pure YAG hot-pressed at 1500 °C was

238 MPa; YAG sintered at 1400 °C by the SPS method reached 348 MPa. The higher matrix strength of the SPS samples could bear the residual stresses resulting from the addition of SiC particles, demonstrating that integrated dense nanocomposites are obtainable by the SPS method.

Because YAG ceramics have a HP temperature similar to that of Al_2O_3 ceramics, the HP temperature of Al_2O_3 -5 vol.% SiC nanocomposites can be used as a reference for the HP temperature of YAG-5 vol.% SiC nanocomposites. Almost all studies on Al_2O_3 -SiC nanocomposites report that the HP temperature for Al_2O_3 -5 vol.% SiC is ~ 1700 °C.^{4,10,14} Thus, the SPS method can lower the densification temperature for YAG-SiC nanocomposites.

3.2. Mechanical properties

Fig. 3 shows the relationship between the mechanical properties and SPS temperature of SPS YAG-SiC and SPS YAG. As shown, the bending strength of YAG-5 vol.% SiC sintered by SPS at 1550 °C can reach 565 MPa, higher than the strength of pure YAG ceramics sintered by HP or SPS. According to other reports³ and our present experimental results, the bending strength of HP YAG is ~ 240 MPa. The bending strength of YAG ceramics can reach 348 MPa when the SPS method is used with powder prepared by the coprecipitation method. Evidently, the addition of nanoscale-sized SiC particles enhances the YAG matrix. The increased strength is a result of the fine grain size and the residual stress produced by the different thermal expansion coefficients of the YAG and SiC.

3.3. Microstructure

Fig. 4 shows SEM photographs of the fracture surfaces of HP YAG, SPS YAG, HP YAG-SiC, and SPS YAG-SiC. Both the transgranular and the intergranular fracture modes exist in HP YAG, possibly

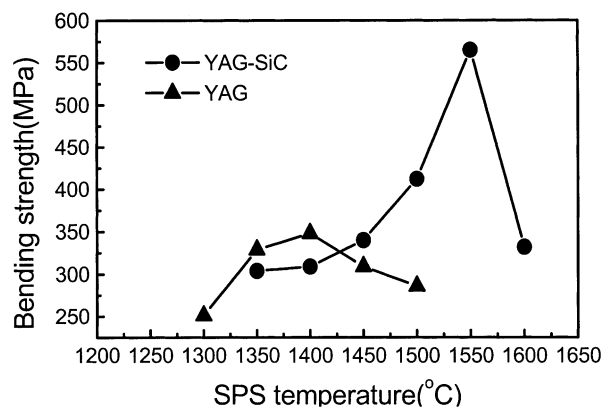


Fig. 3. Bending strength versus sintering temperatures for YAG-5 vol.% SiC nanocomposites sintered by SPS.

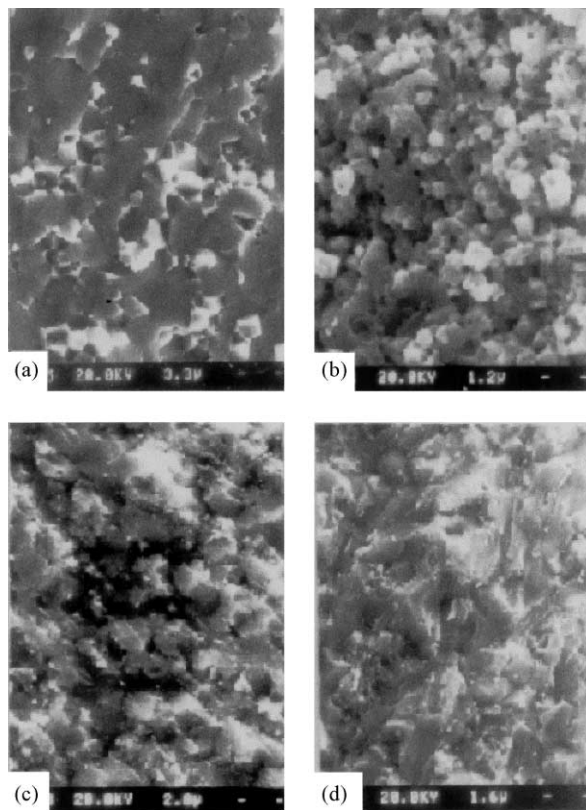


Fig. 4. SEM micrograph of fracture surface of samples: (a) HP YAG, 1500 °C for 1 h; (b) SPS YAG, 1400 °C for 5 min; (c) HP YAG-SiC, 1550 °C for 1 h; (d) SPS YAG-SiC, 1450 °C for 5 min.

because of the weakness of the grain boundary and the matrix. In SPS YAG, the main fracture mode is intergranular, signifying that SPS YAG has stronger grains than does HP YAG, because the strength of the SPS YAG is higher than that of the HP YAG. In HP YAG-SiC and SPS YAG-SiC, the main fracture mode is transgranular. However, the transgranular fracture surface of SPS YAG-SiC has many steps, unlike the flat fracture surface of HP YAG-SiC, revealing that the SPS samples have stronger grains than the HP samples, so that cracks must twist to pass through their YAG grains. The SEM photographs also reveal that the grain size of the HP YAG is $\sim 4 \mu\text{m}$, that of SPS YAG $\sim 1 \mu\text{m}$, and that of SPS YAG-SiC $\sim 2\text{--}3 \mu\text{m}$. The grain size of the SPS YAG is smaller than that of the HP YAG because of a shorter holding time. The grain size of the SPS YAG-SiC is difficult to evaluate from the SEM photographs because of complete transgranular fracture.

Fig. 5 shows TEM photographs of SPS YAG-SiC. The grain size of the YAG is $\sim 1 \mu\text{m}$, indicating that the SPS method produces a finer microstructure than does the HP method. SiC particles are located within the YAG grains, indicating that intragranular YAG-SiC nanocomposites have been obtained. According to residual-stress calculations,^{4,13} this type of intragranular

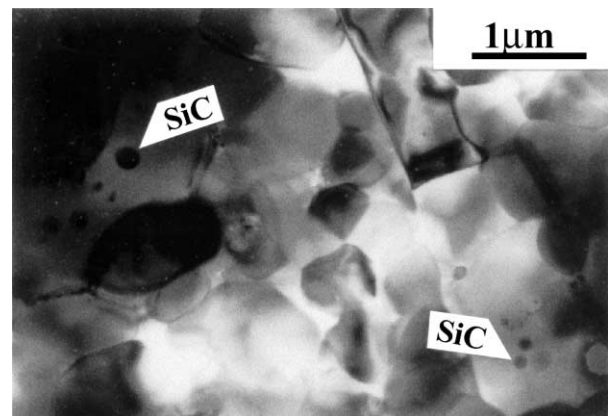


Fig. 5. TEM micrograph of 5 vol.% SiC-YAG sintered by SPS at 1500 °C.

microstructure, in which second-phase particles are located within the matrix grains, is effective for improving strength.

4. Conclusions

Dense bodies of YAG-5 vol.% SiC nanocomposites can be obtained by the SPS method at 1500 °C. The bending strength of those bodies can reach 565 MPa, higher than that of pure YAG. Microstructural observation shows that the fracture mode in SPS YAG-5 vol.% SiC nanocomposites is transgranular. The YAG grain size is $\sim 1 \mu\text{m}$, and SiC particles are located within the YAG grains. Thus, YAG-SiC nanocomposites have stronger grain boundaries than those of pure YAG, and the SPS method is effective for producing YAG-SiC nanocomposites with a fine matrix grain size and an intragranular microstructure.

References

- Parthasarathy, T. A., Mah, T. and Keller, K., Creep mechanism of polycrystalline yttrium aluminum garnet. *J. Am. Ceram. Soc.*, 1992, **75**, 1756–1759.
- Corman, G. S., High-temperature creep of some single crystal oxides. *Ceram. Eng. Sci. Proc.*, 1991, **12**, 1745–1766.
- Keller, K., Mah, T. and Parthasarathy, T. A., Processing and mechanical properties of polycrystalline $\text{Y}_3\text{Al}_5\text{O}_{12}$. *Ceram. Eng. Sci. Proc.*, 1990, **12**, 1122–1133.
- Niihara, K., Nakahira, A. and Sekino, T., New nanocomposite structural ceramics. In *Materials Research Society Symposium Proceedings*, Vol. 286, *Nanophase and Nanocomposite Material*, ed. S. Komarneni, J. C. Parker and G. J. Thomas. Materials Research Society, Pittsburgh, Pennsylvania, 1992, pp. 405–412.
- Tokida, M., Trends in advanced SPS spark plasma sintering system and technology. *J. Soc. Powder Technol. Jpn.*, 1993, **30**, 790–804.
- Gao, L., Shen, Z. J., Miyamoto, H. and Nygren, M., Superfast densification of oxide/oxide ceramic composites. *J. Am. Ceram. Soc.*, 1999, **82**, 1061–1063.
- Gao, L., Wang, H. Z., Hong, J. S., Miyamoto, H. and Nishikawa, Y., Mechanical properties and microstructure of nano-

- SiC–Al₂O₃ composites densified by spark plasma sintering. *J. Euro. Ceram. Soc.*, 1999, **19**, 609–713.
8. Murakami, T., Kitahara, A., Koga, Y., Kawahara, M., Inui, H. and Yamaguchi, M., Microstructure of Nb–Al powders consolidated by spark plasma sintering process. *Mater. Sci. Eng. A*, 1997, **239–240**, 672–679.
 9. Takano, Y., Komeda, T., Yoshinaka, M., Hirota, K. and Yamaguchi, O., Fabrication, microstructure, and mechanical properties of Cr₂O₃/ZrO₂(2.5Y) composite ceramics in the Cr₂O₃-rich region. *J. Am. Ceram. Soc.*, 1998, **81**, 2497–2550.
 10. Wang, H. Z., Gao, L., Gui, L. H. and Guo, J. K., Preparation and properties of intragranular Al₂O₃–SiC nanocomposites. *NanoStruct. Mater.*, 1998, **10**, 947–953.
 11. Wang, H. Z., Gao, L. and Niihara, K., Synthesis of nanoscaled yttrium aluminum garnet powder by the co-precipitation method. *Mater. Sci. Eng. A*, 2000, **288**, 1–4.
 12. Takeuchi, T., Tabuchi, M., Kageyama, H. and Suyama, Y., Preparation of dense BaTiO₃ ceramics with submicrometer grain by spark plasma sintering. *J. Am. Ceram. Soc.*, 1999, **82**, 939–943.
 13. Levin, I., Kaplan, W. D. and Brandon, D. G., Effect of SiC submicrometer particle size and content on fracture toughness of alumina–SiC nanocomposites. *J. Am. Ceram. Soc.*, 1995, **78**, 254–256.
 14. Zhao, J., Stearns, L., Harmer, M. P., Chan, H. M. and Miller, G. A., Mechanical behavior of alumina–silicon carbide nanocomposites. *J. Am. Ceram. Soc.*, 1993, **76**, 503–510.